JOURNAL OF PROPULSION AND POWER
Vol. 14, No. 6, November–December 1998

Spot Mode Transition and the Anode Fall of Pulsed Magnetoplasmadynamic Thrusters

Kevin D. Diamant,* Edgar Y. Choueiri,† and Robert G. Jahn‡
Princeton University, Princeton, New Jersey 08544

An experimentally based description of the major mechanism regulating the anode fall of a high-power, pulsed, self-field magnetoplasmadynamic thruster is presented. Plasma property data recorded to within one electron Larmor radius of the anode indicate that, with increasing current, the anode transitions from a diffuse, low-anode fall mode of operation to a mode with high-anode falls and spotty current attachment. The transition is marked by an order of magnitude increase in ion saturation current noise measured in the anode region, which is attributed to spot motion and, for the case of a smooth anode surface, is triggered by the condition at which the discharge current density to the anode exceeds the random thermal electron current density. Experiments with a roughened anode indicate that the anode fall in the spot mode serves the purpose of evaporating anode material, and comparison of anode falls measured with smooth copper, aluminum, and molybdenum anodes shows that the magnitude of the anode fall in the spot mode is dependent on anode thermal properties. The spot mode is also found to provide an explanation for anode fall saturation.

Nomenclature

J = total thruster current, A
j = discharge current density, A/cm^2
j_{th} = random thermal electron current density, A/cm^2
M = propellant atomic mass, kg
$\dot{m}$ = propellant mass flow rate, kg/s
m_e = electron mass, kg
n = plasma density, m^{-3}
q = elementary charge, C
r_a = radius of current attachment at anode, m
r_c = radius of current attachment at cathode, m
T_e = electron temperature, eV
ε_i = propellant first ionization potential, eV
μ_0 = permeability of free space
ξ = ratio of thruster current to critical ionization current

Introduction

HIGH-power magnetoplasmadynamic (MPD) thrusters offer high-thrust density (10^4–10^5 N/m^2) at specific impulses in the range of 1000–5000 s and have been shown to be advantageous for a number of near-Earth and interplanetary missions.[1–5] In general, these mission studies assume efficiencies of at least 50% over mission times between 1000 and 10,000 h, capabilities that have yet to be demonstrated with gaseous propellants.[6] Major performance limiters with regard to efficiency are frozen flow and anode losses, and even though the fraction of thruster power deposited in the anode can be as low as 10–20% for operation at a few megawatts,[7,8] anode heat fluxes of several kW/cm^2 (Ref. 9) represent a serious problem for anode lifetime. The primary mechanism for anode power deposition is electron current conduction, and the dominant contributor to the energy of electrons entering the anode is the anode fall.

In this paper we present data that indicate the presence of two modes of anode current attachment, the diffuse and spot modes. The anode fall is shown to be a Debye-sheath phenomenon, with mode transition occuring on a smooth anode at sheath current saturation. Mode transition is accompanied by abrupt increases in the anode sheath voltage and in thruster terminal noise, phenomena generally associated with what has been widely termed onset in the MPD thruster anode literature.[10–12] An explanation for the source of the noise and for the behavior of the anode fall is provided.

Facility and Diagnostics

The quasisteady MPD thruster was housed in a cylindrical Plexiglass tank of volume 1.12 m^3 with an i.d. of 0.91 m. Prior to thruster firing, the tank was pumped down to approximately 0.04 Pa (3×10^{-4} torr) by a 15-cm oil diffusion pump and two mechanical pumps. Power was supplied to the thruster by a 160 kJ LC pulse-forming network capable of producing a rectangular current pulse of up to 52 kA for 1 ms.

The thruster (Fig. 1) consisted of a cylindrical plate anode made of copper, aluminum, or molybdenum, and a 2% thoriated tungsten cathode. The inner radius of the anode was machined to a semicircular lip. Equal amounts of argon propellant were injected through 12 equispaced 3-mm-diam holes at a radius of 3.8 cm in the boron nitride backplate and through an annulus surrounding the cathode.

Plasma properties were measured exclusively at the anode lip with triple langmuir and magnetic induction probes. Triple-probe position relative to the anode was determined by imaging the gap between the probe tip and anode with a Questar QM1 microscope–telescope. Limitations of optical access required that triple-probe measurements be taken on the downstream side of the anode lip as shown in Fig. 2. The magnetic induction probe was simply placed directly adjacent to the anode surface at the desired location along the anode lip, so that the probe coil stood approximately 1 mm from the anode surface.

Triple-probe data were reduced with the help of the numerical calculations of Laframboise.[13] Use of Laframboise's calculations in place of the Bohm criterion properly accounts for finite sheath thickness and ion temperature, and, in this study,

Received Aug. 17, 1995; revision received April 19, 1998; accepted for publication June 17, 1998.

*Graduate Student, Electric Propulsion and Plasma Dynamics Laboratory, Department of Mechanical and Aerospace Engineering; currently Technical Staff Member, Hughes Space and Communications Company, Building 230, M/S 1115, 3100 West Lomita Boulevard, Torrance, CA 90505. Member AIAA.

†Chief Scientist and Manager, Electric Propulsion and Plasma Dynamics Laboratory. Member AIAA.

‡Professor, Electric Propulsion and Plasma Dynamics Laboratory, Department of Mechanical and Aerospace Engineering, Fellow AIAA.

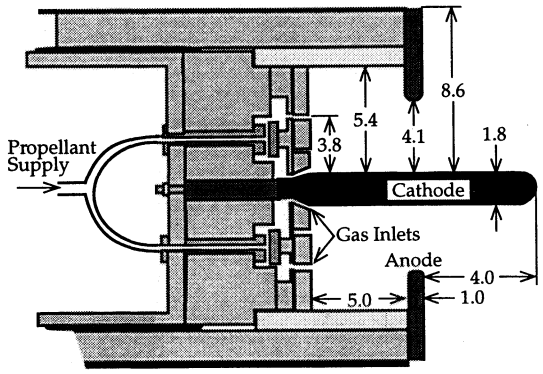

Fig. 1 MPD thruster (dimensions in cm).

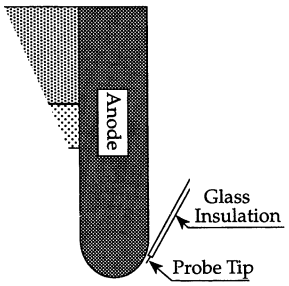

Fig. 2 Triple probe orientation at anode lip.

generally resulted in about a 10% adjustment to properties calculated using the Bohm criterion.

To construct a triple probe with 0.1-mm resolution, three 0.064-mm-diam tungsten wires were individually and then collectively coated with glass by heating and drawing glass tubes over them. The probe tip was trimmed with hydrofluoric and nitric acids. The finished probe had a tip length (length of exposed tungsten wires) of 0.94 mm with a separation between adjacent wires of about one wire radius (the Debye length for all conditions studied was on the order of 1 μm). The three wires lay in the same plane to ensure that they would be equidistant from the anode. A tip length of 0.94 mm results in an uncertainty in the probe position relative to the anode as a result of anode lip curvature that is approximately the same as the uncertainty associated with the finite radius of the probe wires. An additional contribution to positioning uncertainty arises from the uncertainty in the magnification provided by the Questar, which is taken to be 2%. The relative positioning uncertainty when the probe is nominally 0.1 mm from the anode is then 66%.

A magnetic induction probe with a resolution of 1 mm was constructed by wrapping 40 turns of 0.046-mm-diam copper wire around a 0.87-mm-diam alumina core. The coil was protected from the discharge by a rectangular glass sleeve with an exterior width of 2 mm.

Error Bars

Error bars shown in this paper are determined through the application of standard formulas for the propagation of measurement uncertainties.[14] The measurement uncertainties themselves are determined in the following manner: during a thruster pulse, approximately 1000 data points are collected for each measured quantity, and standard deviations are calculated. Each measurement is repeated three to six times, and the final measurement uncertainty is taken to be the average of the standard deviations of each of the trials.

Results and Discussion

Mode Transition

Plasma Properties

Values of the plasma potential with respect to anode potential recorded at 0.1 mm from the anode lip are shown in Fig. 3a (potentials are negative with respect to the anode, representing electron attracting anode falls) as a function of ξ, a parameter defined by Choueiri et al.[15] as the ratio of the thruster current to the current at which the electromagnetic thrust is equal to the product of the mass flow and the propellant critical ionization velocity:

$$\xi = \left(\frac{J^2}{\dot{m}} \frac{\mu_0 \, \ell n(r_a/r_c)}{4\pi (2\varepsilon_i/M)^{1/2}} \right)^{1/2} \tag{1}$$

A discussion of the merit of ξ as a scaling parameter may be found in Ref. 10. The actual operating conditions correspond to mass flow rates of 4 g/s Ar at currents of 8, 12, 16, and 20 kA, and 6 and 16 g/s Ar at 8, 12, 16, 20, and 24 kA, power levels are from 320 kW to 4 MW. The measured values of plasma potential are expected to represent potential differences across a Debye-scale sheath (Debye length on the order of 1 μm) at the anode surface because estimates of the electron Larmor radius based on magnetic field measurements taken 1 mm from the anode surface and temperature measurements 0.1 mm from the surface (Fig. 4) vary from 0.1 to 0.5 mm for the

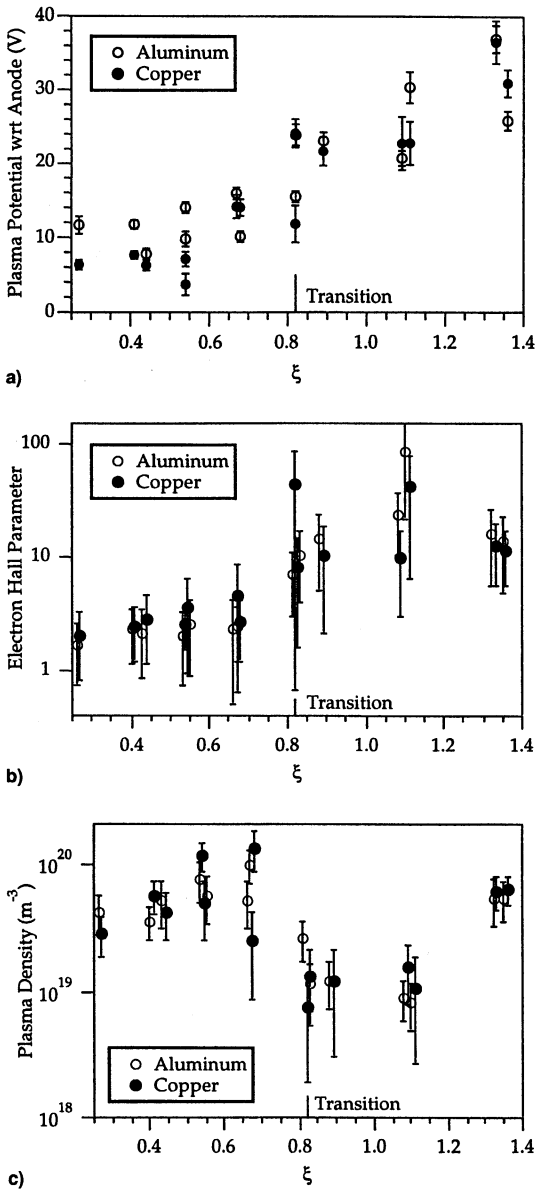

Fig. 3 a) Plasma potential at 0.1 mm, b) electron Hall parameter at 0.5 mm, and c) plasma density at 0.1 mm for aluminum and copper anodes.

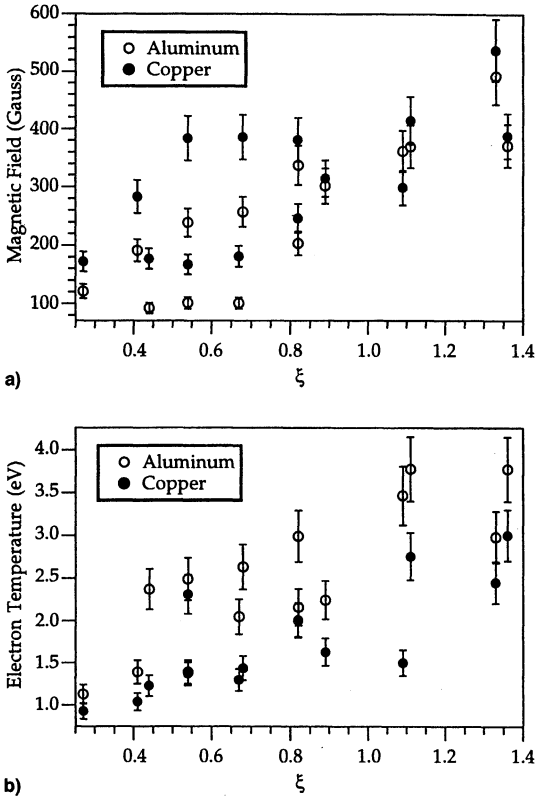

Fig. 4 a) Magnetic field at 1 mm and b) electron temperature at 0.1 mm for aluminum and copper anodes.

operating conditions shown, and estimates of the electron–ion mean free path are larger than the electron Larmor radius by the factors shown in Fig. 3b electron Hall parameters). At a ξ value of approximately 0.8, a transition is observed from operation with sheath potentials below 16 V to conditions in which the sheath potential assumes values between 20 and 40 V. This transition corresponds to the sudden appearance of large values of the electron Hall parameter (Fig. 3b) and an abrupt decrease in plasma density (Fig. 3c). The resurgence of the plasma density for $\xi > 1.3$ will be discussed later. Some data points in Figs. 3b and 3c have been shifted in ξ value by 0.01 or less to clarify error bar placement.

Noise

The transition is also marked by an abrupt increase in discharge noise. A survey of ion saturation current fluctuations near the anode was conducted for ξ values from 0.44 to 1.33 at a mass flow rate of 6 g/s (currents of 8, 12, 16, 20, and 24 kA). In general, the frequency content of these fluctuations is dominated by broad noise in the range of 100–500 kHz. In addition, smaller peaks are often present at frequencies of approximately 2, 3, 4, and 7 MHz (the Nyquist frequency of the experiment was 10 MHz). Figure 5 shows amplitudes of a number of these peaks (arbitrary units) normalized by the dc level of the ion saturation current as a function of distance from the (aluminum) anode surface. In the interest of simplicity, a distinction is made only between peaks observed at ξ values above transition and those below transition, regardless of peak center frequency. Two things are evident from this figure. The first is that the noise level increases monotonically as the anode surface is approached, indicating that the source of the noise is close to the anode surface. The second is that the noise at conditions above mode transition is an order of magnitude or more greater than for those below transition. Figure 6a plots the noise peaks at 0.1 mm shown in Fig. 5 as a function of ξ along with similar data obtained with a copper anode. It is interesting to note that the copper anode appears

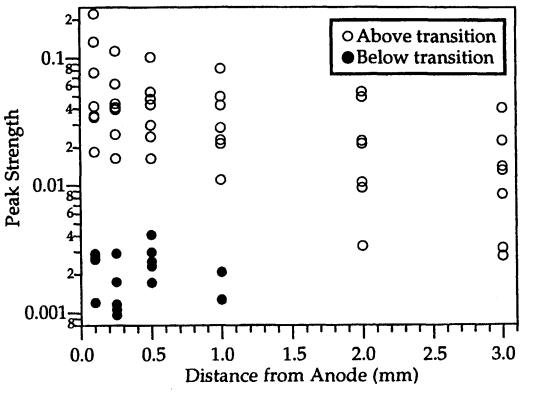

Fig. 5 Amplitudes of 2-, 3-, 4-, and 7-MHz peaks in ion saturation current noise for ξ values above and below transition near aluminum anode.

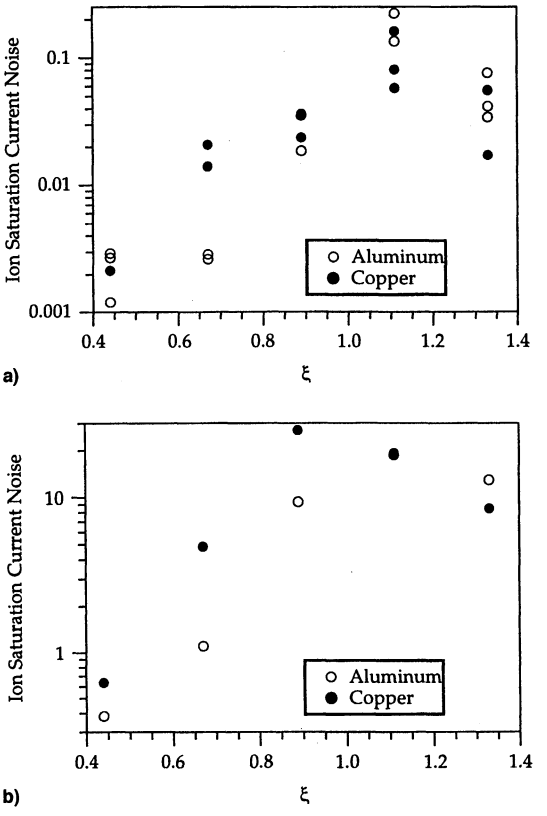

Fig. 6 Ion saturation current noise (arbitrary units) at 0.1 mm from aluminum and copper anodes: a) peak amplitudes and b) integrated over 50 kHz to 2 MHz.

to transition at a lower ξ value than the aluminum. This is also evident in Fig. 6b, in which data points are obtained by integrating noise spectra recorded at 0.1 mm over the range from 50 kHz to 2 MHz, followed by normalization with the dc current level (error bars are not presented for this highly qualitative data). The apparent early transition of copper will be demonstrated again shortly and discussed in connection with results obtained with the molybdenum anode.

Spot Mode

Vacuum Arcs and Spot-Induced Noise

Anode mode transition is a widely observed and well-documented phenomenon in vacuum arcs.[16] The transition from a diffuse current attachment to one in which arc spots are present on the anode surface is marked by a sudden increase in the arc terminal voltage and in terminal voltage fluctuations.[17] Har-

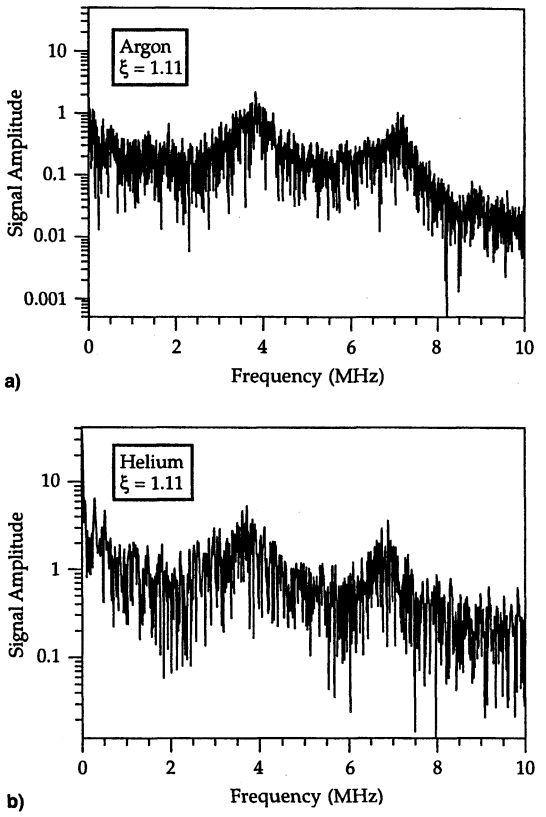

Fig. 7 Nonnormalized ion saturation current noise spectra at 0.1 mm from aluminum anode for $\xi = 1.11$: a) argon and b) helium.

ris[18] has demonstrated a direct link between terminal noise and the appearance of transient luminous spots on the anode of a vacuum arc with copper electrodes. Harris also shows that the frequency of oscillations in luminosity corresponds directly to the frequency of terminal voltage fluctuations, and is insensitive to variations in arc current.

We consider the noise observed near our thruster anode to be the result of spot motion. Comparison of ion saturation current fluctuation spectra recorded with argon and helium propellants at the same values of ξ show no appreciable differences in MHz level frequency content (Fig. 7), indicating that it is unlikely that the noise originates from a natural plasma oscillation because oscillations at frequencies of a few MHz in our plasma would very likely be dependent upon ion mass.

Similar results have been obtained by Kuriki and Iida,[19] who found that voltage fluctuation spectra recorded with argon and hydrogen were nearly identical in the MHz range. Theories regarding the motion of spot current attachments on cathodes generally invoke interactions between the spot current and magnetic fields induced by the global discharge current and/or by the local spot current, and are independent of ion mass.[20,21]

Physical Evidence for Spot Mode

To test the spot hypothesis, a simple experiment was run in which polished anodes were observed before and after 10 thruster firings at the same conditions used in the noise experiment (ξ from 0.44 to 1.33 at 6 g/s mass flow). Spot damage visible to the unaided eye (craters or abrasions on the order of 1 mm in diameter) was evident for the posttransition ξ values of 0.89, 1.11, and 1.33, but not for the pretransition values of 0.44 and 0.67 with aluminum and copper anodes.[22] Spot damage was found almost exclusively on the anode lip. Spectroscopic erosion studies performed on the same thruster used in our work confirm that emission lines corresponding to anode material (aluminum) appear at a current of 16 kA when the thruster is fed 6 g/s argon ($\xi = 0.89$) with a propellant mass distribution similar to ours.[23]

Trigger for Transition

It has been postulated that the ratio of j to j_{th} governs anode mode transition.[24–26] Because the anode fall is largely a Debye-sheath phenomenon, we can look to langmuir probe theory, which tells us that the current collected by a planar conductor (the ratio of the anode lip radius to Debye length is approximately 5000) immersed in a quiescent plasma saturates at a level approximately equal to the random thermal current. Attempts to collect larger currents result in very large increases in the collector potential relative to the plasma, and corresponding increases in the energy input to the collector surface. At some point the input energy becomes sufficient to cause local overheating and the significant evaporation of collector material. Following ionization by incoming electrons, this material contributes to an increase in current to the evaporative region, leading to enhanced evaporation. This *runaway* effect results in spot formation.[27]

Discharge current densities varying from about 100 to 400 A/cm^2 have been calculated through the application of Ampere's law to magnetic field measurements made along the lip (at positions straddling the location of the triple-probe measurements) of copper and aluminum anodes at a distance of approximately 1 mm from the anode surface, and are shown in Fig. 8 (some data points have been shifted in ξ value by 0.01 or less to clarify error bar placement) normalized by j_{th} calculated from n and T_e measured 0.1 mm from the anode

$$j_{th} = nq(qT_e/2\pi m_e)^{1/2} \tag{2}$$

Figure 8 shows that indeed for the conditions below transition ($\xi < 0.8$), the ratio j/j_{th} is close to 1 (except for copper at $\xi = 0.67$), whereas at the point of transition, values from 3 to 10 are achieved. With increases in ξ, the ratio returns to 1, because of the previously mentioned resurgence in plasma density.

In Fig. 8 the data point corresponding to the copper anode operating at $\xi = 0.67$ indicates that mode transition should have occurred at that operating condition. During the polished anode experiment, the copper anode did not show visible damage after 10 firings at $\xi = 0.67$. However, as previously mentioned, there is evidence for transition in the noise data, and careful inspection of Fig. 3a reveals that the anode fall for $\xi = 0.67$ lies midway between other values recorded before and after transition. Further evidence for the material dependence of transition will be presented in conjunction with the discussion of the behavior of the molybdenum anode.

Resurgence of Plasma Density and j_{th}

As mentioned previously, j/jth returns to values near 1 at $\xi > 1.3$, presenting us with an apparent contradiction. We can

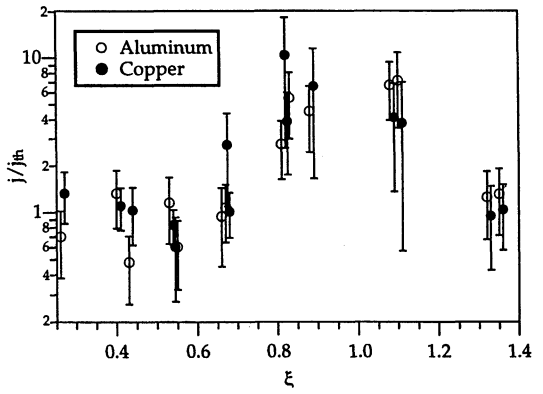

Fig. 8 Ratio of discharge to thermal current density.

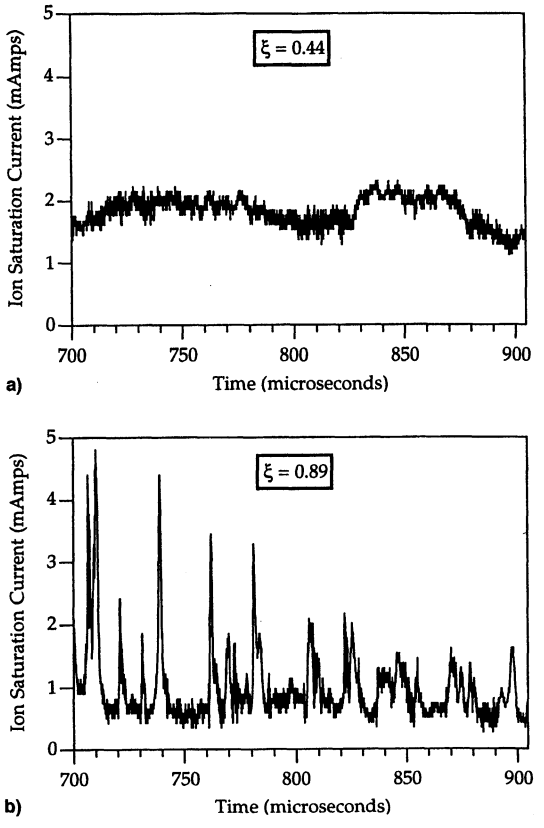

Fig. 9 Ion saturation current time histories for ξ = a) 0.44 and b) 0.89 with aluminum anode.

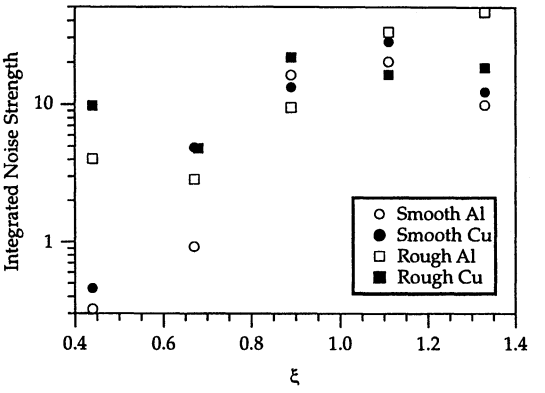

Fig. 10 Integrated ion saturation current noise (50 kHz to 2 MHz) 0.25 mm from rough and smooth aluminum and copper anodes.

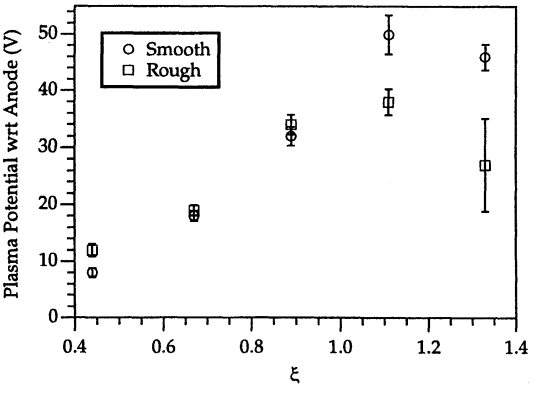

Fig. 11 Plasma potential a few millimeters from smooth and roughened aluminum anodes.

provide the following explanation in terms of how the spot mode develops and the manner in which plasma properties were measured. Figure 9a is an unfiltered time history of the ion saturation current collected during a thruster firing at a condition below transition. The trace is quiescent in comparison with the same measurement, shown in Fig. 9b, taken at a condition just above transition.

The trace in Fig. 9b is punctuated, roughly at a frequency of 100 kHz, by excursions up to an order of magnitude larger than the dc level. We attribute these excursions to the passage of spots by the probe location. Further increases in ξ result in traces dominated by the excursions, caused by either enhanced spot motion or an increase in the number of spots. The probe used to measure the ion saturation current is equipped with a filter that heavily attenuates signals in the range of 100 kHz. As a result, the intermittent excursions of Fig. 9b are squelched, and the recorded values will reflect the low-density plasma outside of the spots. With increasing ξ, the more intense spot vapor production results in probe readings which, after filtering and averaging, display the net effect of the spot action, which is to solve the starvation crisis.

Experiments with a Roughened Anode

In an attempt to produce a condition that would favor transition by providing preferential points of attachment, a knurling tool was run over the anode surface, producing roughness on a scale of approximately 0.1 mm. Inspection of roughened aluminum and copper anodes before and after 10 thruster firings at all of the conditions studied (ξ values of 0.44, 0.67, 0.89, 1.33, and 1.36 with 6 g/s argon mass flow) indicated the presence of the spot mode.

Inducing the spot mode impacted both the thruster noise level and anode fall. Figure 10 is a comparison of integrated noise (over the range from 50 kHz to 2 MHz) for the smooth and roughened anodes.

For conditions in which the smooth anodes did not transition, the roughened anodes exhibit significantly more noise, by an order of magnitude at ξ = 0.44. This is further evidence that the noise accompanying transition is directly associated with the spots. Figure 11 shows plasma potentials measured a few millimeters from smooth and roughened aluminum anodes as a function of ξ.

At low values of ξ, the roughened anode fall exceeds that of the smooth anode by a few volts, perhaps because of the increased plasma resistivity produced by the excessive evaporation of anode material. At the two highest values of ξ, however, the anode fall is substantially decreased.

Anode Fall and Anode Vaporization

An explanation for the reduced anode falls obtained with roughened anodes appears quite readily if it is presumed that the anode fall in the spot mode is established by the minimum input power required to heat the anode surface to the point where significant evaporation of anode material occurs. For a given input power, metal whiskers produced by the roughing will reach higher temperatures at their extremities because of the low cross-sectional area of heat conduction paths into the body of the anode (power input to the whiskers is probably also enhanced by local electric field concentrations). Lower anode falls are thus required to achieve temperatures required for significant vaporization. This, of course, also explains why the roughened anodes transition at smaller ξ values, because they allow vaporization even at the low input power available from a sheath that has not yet reached current saturation. Smooth anodes, on the other hand, appear to require the increased power available from the large increases in sheath voltage that accompany current saturation.

An attempt to quantify what anode temperatures should be required for significant vaporization may be made by adopting the criterion that the temperature should be such that the equilibrium vapor density of the anode material is comparable to

measured values of the plasma density near the anode.[26] For the copper and aluminum anodes the resulting values are approximately 1400 K. Two points can be made with regard to this value. The first is that the melting points of aluminum and copper are 934 and 1357 K, respectively. This is in accord with experimental observations of gross melting associated with spot attachments on the aluminum anode, where material has clearly been splashed about. Gross melting, however, was never observed on the copper anode. The second point is that if we very simplistically model the anode as a semi-infinite solid with a constant applied heat flux (determined by the product of current density with the anode fall, electron enthalpy, and surface work function), then we find that to obtain surface temperatures near 1400 K in the course of a 1-ms firing with measured values of the anode fall and electron temperature, we must require constriction of the current density to approximately 2000 A/cm^2, which is almost an order of magnitude larger than typical values measured 1 mm from the anode surface. This is, of course, in accord with the spot hypothesis and with the size of the excursions in the ion saturation current shown in Fig. 9b.

Experiments with a Molybdenum Anode

Anode Fall

Data regarding the material dependence of the anode fall lead naturally to the conclusion that low-vapor-pressure anode materials should exhibit larger anode falls in the spot mode. A molybdenum anode was chosen to test this hypothesis. Equilibrium vapor pressure data for molybdenum indicate that a temperature near 2800 K is required to produce vapor densities comparable to plasma densities measured near copper and aluminum anodes. Application of the simple heat transfer model described previously, with an assumed spot current density of 2000 A/cm^2, indicates that anode falls in excess of 80 V might be expected. Values this large were not observed; however, it is clear from Fig. 12 that for conditions above transition, anode falls measured with the molybdenum anode exceed those with copper and aluminum anodes by a substantial margin. Accurate determination of spot current densities (which would provide more reliable estimates of required anode falls), is a difficult task that has received considerable attention with regard to cathode spots, for which published values can vary by several orders of magnitude.[28]

Early Transition

The molybdenum anode also transitions at a lower value of ξ than do the copper and aluminum anodes. As previously mentioned, noise and anode fall data with the copper anode at $\xi = 0.67$ seemed to indicate transition in progress; however, no damage visible to the unaided eye was observed on the anode surface. In contrast, physical damage was observed on the molybdenum anode after operation at $\xi = 0.67$. Much like

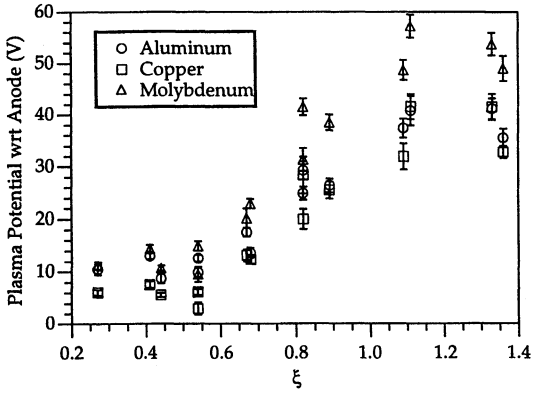

Fig. 12 Plasma potential 0.5 mm from aluminum, copper, and molybdenum anodes.

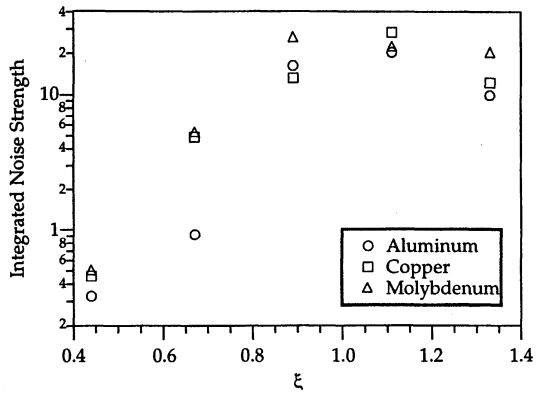

Fig. 13 Integrated ion saturation current noise (50 kHz to 2 MHz) 0.25 mm from aluminum, copper, and molybdenum anodes.

the copper anode, this damage did not involve gross anode melting, in accordance with the estimated surface temperature requirement (2800 K) lying below the melting point of molybdenum (2896 K). The transition is marked by the appearance of anode falls in excess of 20 V (Fig. 12) and an order of magnitude increase in ion saturation current noise as compared to operation at $\xi = 0.44$ (Fig. 13).

The material dependence of the point of transition may arise from anode erosion in the diffuse mode. The relatively higher vapor pressure of aluminum at low temperature may supply the discharge with sufficient material to postpone the criticality of j/j_{th} to higher ξ values than for copper or molybdenum.

Anode Fall Saturation

A final observation may be made with regard to another very widely observed and well-documented behavior in vacuum arcs, namely that with increasing current after transition, the arc noise level and arc terminal voltage both decrease substantially, presumably because of the intense spot attachment with prolific vapor generation.[17] This behavior is observed in the data of Figs. 3a, 6a, 6b, 10, 12, and 13, which show that the anode fall and near-anode noise level reach a peak and then decrease at the highest ξ values studied. Other researchers have observed anode fall saturation[9,29] and Gallimore[9] has associated it with the decrease of the anode power fraction with increasing thruster power. The spot mode provides a plausible explanation for anode fall saturation.

Conclusions

Plasma properties near the aluminum and copper anodes of a high-power-pulsed MPD thruster indicate that the anode current collection transitions from a diffuse, low-voltage, and low-noise mode to one of high-voltage, high-noise, and spotty current attachment. The mode transition is triggered by anode sheath current saturation, which results in increasing power to the anode surface until local heating and vaporization generate spots, resulting in a limitation of the anode sheath voltage to values required to vaporize sufficient anode material to solve the starvation crisis. Premature induction of the spot mode accomplished by roughening the anode surface confirms that the increased discharge noise associated with this mode is generated by the arc spots, and that anode vaporization controls the anode fall voltage in the spot mode. Experiments with a molybdenum anode confirm the expectation that anode falls in the spot mode should increase as the anode material becomes more refractory. Finally, the spot mode is found to provide an explanation for anode fall saturation and the consequent decrease of the anode power fraction with increasing thruster power.

Acknowledgments

This work has been supported in part by the Fannie and John Hertz Foundation. The authors thank George E. Miller for his invaluable assistance in the laboratory.

References

[1]Gilland, J. H., "Mission and System Optimization of Nuclear Electric Propulsion Vehicles for Lunar and Mars Missions," 22nd International Electric Propulsion Conf., Paper 91-038, Oct. 1991.

[2]Sercel, J., and Krauthamer, S., "Multimegawatt Nuclear Electric Propulsion; First Order System Design and Performance Evaluation," AIAA Paper 86-1202, June 1986.

[3]King, D. Q., and Sercel, J. C., "A Review of the Multi-Megawatt MPD Thruster and Current Mission Applications," AIAA Paper 86-1437, June 1986.

[4]Rudolph, L. K., and Hamlyn, K. M., "A Comparison Between Advanced Chemical and MPD Propulsion for Geocentric Missions," AIAA Paper 83-1391, June 1983.

[5]Choueiri, E. Y., Kelly, A. J., and Jahn, R. G., "Mass Savings Domain of Plasma Propulsion for LEO to GEO Transfer," *Journal of Spacecraft and Rockets*, Vol. 30, No. 6, 1993, pp. 749–754.

[6]Sovey, J. S., and Mantenieks, M. A., "Performance and Lifetime Assessment of Magnetoplasmadynamic Arc Thruster Technology," *Journal of Propulsion and Power*, Vol. 7, No. 1, 1991, pp. 71–83.

[7]Oberth, R. C., "Anode Phenomena in High-Current Discharges," Ph.D. Dissertation, Princeton Univ., Princeton, NJ, Dec. 1970.

[8]Saber, A. J., "Anode Power in a Quasi-Steady MPD Thruster," Ph.D. Dissertation, Princeton Univ., Princeton, NJ, May 1974.

[9]Gallimore, A. D., "Anode Power Deposition in Coaxial MPD Thrusters," Ph.D. Dissertation, Princeton Univ., Princeton, NJ, Oct. 1992.

[10]Diamant, K. D., "The Anode Fall in a High Power Pulsed MPD Thruster," Ph.D. Dissertation, Section 1.3, Princeton Univ., Princeton, NJ, June 1996.

[11]Barnett, J. W., and Jahn, R. G., "Onset Phenomena in MPD Thrusters," AIAA Paper 85-2038, Sept. 1985.

[12]Rudolph, L. K., Jahn, R. G., Clark, K. E., and Von Jaskowsky, W. F., "Onset Phenomena in Self-Field MPD Arcjets," AIAA Paper 78-653, 1978.

[13]Laframboise, J. G., "Theory of Spherical and Cylindrical Langmuir Probes in a Collisionless Maxwellian Plasma at Rest," TR 100, Univ. of Toronto Inst. for Aerospace Studies, Toronto, ON, Canada, 1966.

[14]Bevington, P. R., *Data Reduction and Error Analysis for the Physical Sciences*, McGraw–Hill, New York, 1969, p. 64.

[15]Choueiri, E. Y., Kelly, A. J., and Jahn, R. G., "MPD Thruster Plasma Instability Studies," Paper AIAA 87-1067, May 1987.

[16]Miller, H. C., "A Review of Anode Phenomena in Vacuum Arcs," *IEEE Transactions on Plasma Science*, Vol. 13, No. 5, 1985, pp. 242–252.

[17]Mitchell, G. R., "High-Current Vacuum Arcs: Part I—An Experimental Study," *Proceedings of the Institution of Electrical Engineers*, Vol. 117, No. 2, 1970, pp. 2315–2326.

[18]Harris, L. P., "Small-Scale Anode Activity in Vacuum Arcs," *IEEE Transactions on Plasma Science*, Vol. 10, No. 3, 1982, pp. 173–180.

[19]Kuriki, K., and Iida, H., Spectrum Analysis of Instabilities in MPD Arcjet," 17th International Electric Propulsion Conf., Paper 84-28, 1984.

[20]Schrade, H. O., Auweter-Kurtz, M., and Kurtz, H. L., "Cathode Phenomena in Plasma Thrusters," International Electric Propulsion Conf., May AIAA Paper 87-1096, May 1987.

[21]Harris, L. P., "Transverse Forces and Motions at Cathode Spots in Vacuum Arcs," *IEEE Transactions on Plasma Science*, Vol. 11, No. 3, 1983, pp. 94–102.

[22]Diamant, K. D., Mechanical and Aerospace Engineering Dept., Rept. EPPDyL-TR-95S, Princeton Univ., Princeton, NJ, Jan. 1995.

[23]Ho, D. D., "Erosion Studies in an MPD Thruster," M.S. Thesis, Princeton Univ., Princeton, NJ, May 1981.

[24]Hugel, H., "Effect of Self-Magnetic Forces on the Anode Mechanism of a High Current Discharge," *IEEE Transactions on Plasma Science*, Vol. 8, No. 4, 1980, pp. 437–442.

[25]Vainberg, L. I., Lyubimov, G. A., and Smolin, G. G., "High-Current Discharge Effects and Anode Damage in an End-Fire Plasma Accelerator," *Soviet Physics Technical Physics*, Vol. 23, No. 3, 1978, pp. 439–443.

[26]Dyuzhev, G. A., Lyubimov, G. A., and Shkol'nik, S. M., "Conditions of the Anode Spot Formation in a Vacuum Arc," *IEEE Transactions on Plasma Science*, Vol. 11, No. 1, 1983, pp. 36–45.

[27]Lafferty, J. M., "Triggered Vacuum Gaps," *Proceedings of the IEEE*, Vol. 54, No. 1, 1966, pp. 23–32.

[28]Hantzsche, E., and Juttner, B., "Current Density in Arc Spots," *IEEE Transactions on Plasma Science*, Vol. 13, No. 5, 1985, pp. 230–234.

[29]Kuriki, K., and Onishi, M., "Thrust Measurement of K III MPD Arcjet," AIAA Paper 81-0683, April 1981.